Early stages of retinal development depend on Sec13 function

Katy Schmidt[1,*,‡], Florencia Cavodeassi[2,§], Yi Feng[1,¶] and David J. Stephens[1]

[1]Cell Biology Laboratories, School of Biochemistry, Medical Sciences Building, University of Bristol, University Walk, Bristol BS8 1TD, UK
[2]Department of Cell and Developmental Biology, University College London, Gower Street, London WC1E 6BT, UK

*Author for correspondence (katy.schmidt@univie.ac.at)
‡Present address: Max F. Perutz Laboratories, University of Vienna and Medical University of Vienna, Dr-Bohr-Gasse 9/3, 1030 Wien, Austria
§Present address: Centro de Biologia, Molecular Servero Ochoa (UAM-CSIC), Nicolas Cabrera 1, Universidad Autonoma de Madrid, Madrid, Spain
¶Present address: MRC Centre for Inflammation Research, QMRI, Little France Crescent, Edinburgh EH16 4TJ, UK

Biology Open 2, 256–266
doi: 10.1242/bio.20133251
Received 2nd October 2012
Accepted 22nd November 2012

Summary

ER-to-Golgi transport of proteins destined for the extracellular space or intracellular compartments depends on the COPII vesicle coat and is constitutive in all translationally active cells. Nevertheless, there is emerging evidence that this process is regulated on a cell- and tissue-specific basis, which means that components of the COPII coat will be of differential importance to certain cell types. The COPII coat consists of an inner layer, Sec23/24 and an outer shell, Sec13/31. We have shown previously that knock-down of Sec13 results in concomitant loss of Sec31. In zebrafish and cultured human cells this leads to impaired trafficking of large cargo, namely procollagens, and is causative for defects in craniofacial and gut development. It is now widely accepted that the outer COPII coat is key to the architecture and stability of ER export vesicles containing large, unusual cargo proteins. Here, we investigate zebrafish eye development following Sec13 depletion. We find that photoreceptors degenerate or fail to develop from the onset. Impaired collagen trafficking from the retinal pigment epithelium and defects in overall retinal lamination also seen in Sec13-depleted zebrafish might have been caused by increased apoptosis and reduced topical proliferation in the retina. Our data show that the outer layer of the COPII coat is also necessary for the transport of large amounts of cargo proteins, in this case rhodopsin, rather than just large cargo as previously thought.

Key words: COPII, Rhodopsin, ER export, Zebrafish, Eye

Introduction

Trafficking of newly synthesised proteins underpins all aspects of cellular function including the generation and maintenance of organelles, and differentiation and morphogenesis of multicellular structures. The rate-limiting first step of secretion is the controlled export of cargo proteins from their site of synthesis in the endoplasmic reticulum (ER) (Kondylis et al., 2009; Schmidt and Stephens, 2010). We know much about the machinery underpinning the structure and function of the early secretory pathway but little of how its components relate to tissue patterning during ontogenesis. Similarly, while a number of trafficking-related human pathologies have been reported (Aridor and Hannan, 2000; Aridor and Hannan, 2002; Boyadjiev et al., 2006; Hughes and Stephens, 2008; Lang et al., 2006) we have a poor understanding of how defects in membrane trafficking lead to developmental malformations or disease states.

ER export of nearly all transmembrane and secretory proteins relies on the function of the COPII complex (Barlowe et al., 1994). COPII assembles on ER exit sites (ERES), specific subdomains of the endoplasmic reticulum (Hughes and Stephens, 2008). Assembly of the protein coat is directed by Sec12-driven activation of the small GTP-binding protein Sar1. Sar1-GTP recruits Sec23/Sec24; this inner layer of COPII is thought to mediate cargo capture. Subsequently, the outer layer of COPII, Sec13/Sec31, assembles on this pre-budding complex and completes vesicle formation (reviewed by Zanetti et al., 2012). *In vitro*, COPII proteins can generate 60–80 nm-sized vesicles on synthetic liposomes (Matsuoka et al., 1998). Similarly sized protein cages can also assemble from purified Sec13/31 (Stagg et al., 2006) or found in, or can be extracted from, cells (Aridor et al., 1999; Matsuoka et al., 2001). More recently, it has been shown that the geometry of the outer layer of the COPII coat is structurally flexible and could be the means by which ER-derived transport vesicles adapt to cargo of different size and shape such as procollagens (O'Donnell et al., 2011; Stagg et al., 2008). Cranio-lenticulo-sutural dysplasia (CLSD), a disease characterised by craniofacial abnormalities, is caused by an accumulation of procollagen within the ER (Fromme et al., 2007). The causal mutation in Sec23 (Boyadjiev et al., 2006) lies at the interface between Sec23 and Sec31 resulting in defective recruitment of Sec13/31 (Bi et al., 2007; Fromme et al., 2007). Other work supports the concept that coupling between inner and outer layers of the COPII coat is essential for procollagen secretion (Bhattacharya et al., 2012; Townley et al., 2008). Indeed, our experiments showed that suppression of Sec13 expression and concomitant loss of Sec31 resulted in craniofacial development defects in zebrafish and, in human cells led to intracellular accumulation of procollagen. Secretion of other, small freely diffusible cargoes, on the other hand, was not affected (Townley et

al., 2008). In addition, Sec13 morphant zebrafish show hypomorphic eyes and impaired intestinal morphogenesis. We have recently characterised the latter and our results indicate a causal link between ER export of large cargo and intestinal morphogenesis in zebrafish and lumen expansion in 3D tissue culture (Townley et al., 2012). Here, we explore the Sec13-dependent eye phenotype.

The optic cup is already well-developed 24 hours post fertilisation (hpf) (Schmitt and Dowling, 1999). At this stage, the rapidly proliferating retina is composed of the retinal pigment epithelium (RPE) and the retinal neuroepithelium. The RPE and the neural retina, namely photoreceptors, develop interdependently. The RPE is initially responsible for correct differentiation of the retina and photoreceptors (Hollyfield and Witkovsky, 1974; Raymond and Jackson, 1995; Stiemke et al., 1994). Maturation of the RPE then depends on the final steps in photoreceptor differentiation (Marmorstein et al., 1998). Differentiation and maintenance of both cell types heavily rely on cargo transport and directed membrane trafficking. For instance, the visual cycle depends on transport and processing of retinoids by the RPE. The RPE has to phagocytose outer segments shed from photoreceptors and transversally transport nutrients, water, electrolytes and waste products. Components of the inter-photoreceptor matrix as well as growth factors are secreted apically whereas proteins destined for the Bruch's membrane are secreted basally. The Bruch's membrane defines the polarity of the RPE. However, a moderately intact Bruch's membrane has been shown to be sufficient to induce RPE differentiation and polarity in wounding experiments (Shiragami et al., 1998).

Photoreceptor cells are morphologically unique; they are divided into an inner segment containing the nucleus and all organelles and an outer segment, a specialised primary cilium, entirely comprised of stacked membrane sheets packed with rhodopsin. Discs from the outer segment are replaced continuously; hence, the transport load for rhodopsin in photoreceptors is very high. Rhodopsin is a seven-pass transmembrane protein, directly inserted into the membrane upon translation at the ER. Many of the secondary modifications of rhodopsin take place in the ER and are a prerequisite for ER export (Murray et al., 2009). Hence, ER export has to play a significant role in eye development and vision. However, most studies involving accumulation of rhodopsin in the ER have concentrated on rhodopsin mutations (Kunte et al., 2012; Saliba et al., 2002; Shinde et al., 2012) or on Golgi to plasma membrane transport (Deretic, 2006; Deretic and Wang, 2012). ER-to-Golgi transport has also not been taken into account in models of rhodopsin transport within the inner segment (Karan et al., 2008).

Here, we analyse ER-to-Golgi transport of endogenous rhodopsin following disruption of COPII vesicle coat function. Consistent with our previous work, we find that in Sec13 morphant zebrafish, in which Sec31 is concomitantly lost, collagen transport from the RPE is reduced and retinal lamination is not established. In addition, we find that rhodopsin trafficking is greatly impaired. We conclude that the outer COPII coat is also necessary for trafficking of large amounts of cargo rather than just large cargo as previously thought.

Results

Sec13 depletion leads to reduced eye size and retinal lamination defects

We have previously shown (Townley et al., 2008) that Sec13 morphant zebrafish embryos have kinked fins and a disrupted craniofacial skeleton at 5 days post fertilisation (dpf). Eyes of 5 dpf morphant fish appeared smaller and misshapen (Townley et al., 2008), but it was unclear whether this could have been a secondary effect to the head skeleton being malformed due to impaired collagen trafficking. Scanning electron microscopy (SEM) at 5 dpf revealed that the retina of Sec13 morphants was greatly reduced in all embryos whereas the lens itself was comparable in size to controls (compare Fig. 1A,G). The external phenotype of the eyes at 5 dpf was generally more diverse than other phenotypic manifestations such as head size or bending of the fins across all examined specimens. 67% of the embryos (30 of 45, Fig. 1G) showed a dramatic reduction of the retina. 13% (6 of 45, Fig. 1G inset) appeared nearly normal and the remaining 20% had an intermediate phenotype. This suggested that the eye phenotype of Sec13 morphants might not be a mere consequence of the malformed head skeleton. Either the eyes could be specifically susceptible to the loss of Sec13, or this variability seen at day 5 of embryonic development could be due to a differential decrease of concentration of morpholino oligonucleotides per cell in the eyes (Bill et al., 2009; Eisen and Smith, 2008; Sumanas and Larson, 2002).

To thoroughly characterise the eyes of Sec13 morphants, control and morphant embryos between 1 dpf and 4 dpf were investigated by SEM (Fig. 1B,C,H,I; data not shown) to define the first appearance of the phenotype. At 4 dpf, head and eye size were already reduced in morphant zebrafish (compare Fig. 1B,H); this was most noticeable by the lack of indentation between retina and lens in Sec13-depleted embryos (Fig. 1H, inset). Kinked fins, craniofacial and eye phenotypes were largely coincident in their severity. The morphant phenotype was more uniform at 4 dpf compared to 5 dpf with 77% of the embryos showing the same phenotype (37 of 48). This supported the idea that the observed variability may be due to differential susceptibility to, or decrease of concentration of, morpholino oligonucleotides. At 3 dpf, the eyes of control and morphant embryos were indistinguishable (compare Fig. 1C,I) although bending of the fins (not shown) and a minor disparity of head size was already recognisable. No apparent difference was observed between morphant and control embryos at 1 and 2 dpf (data not shown). Thus, the external phenotype became morphologically evident between 3 and 4 dpf, therefore histological changes would have had to occur before 3 dpf.

Toluidine Blue staining on resin sections showed that the retina of Sec13 morphants was indeed greatly disrupted at 3 dpf (compare Fig. 1F,L). Maturation of retinal lamination could easily be followed in control samples from 3 dpf (Fig. 1D–F). Between 4 dpf and 5 dpf, the photoreceptor layer differentiated (Fig. 1D,E, arrowheads) and outer segments developed (Fig. 1D,E, compare elongation of dark blue structures). As expected, a small amount of cell death occurred in the eyes of control embryos at 3 dpf (Fig. 1F, star). In contrast, 3 dpf morphant retinae (Fig. 1J) showed a large number of pyknotic nuclei (Fig. 1L, star) and retinal lamination was hardly noticeable. The RPE was hypertrophic with amorphous boundaries (Fig. 1D–F and Fig. 1J–L, compare arrows). Although the retina appeared improved in most examined specimens by 4 dpf, retinal lamination was still largely absent in Sec13 morphants (compare decrease in dark condensed debris with severe example, Fig. 1K, inset). Strikingly, the photoreceptor layer seemed absent and outer segments were not seen in any samples at 4 dpf (Fig. 1E,K, compare arrowheads).

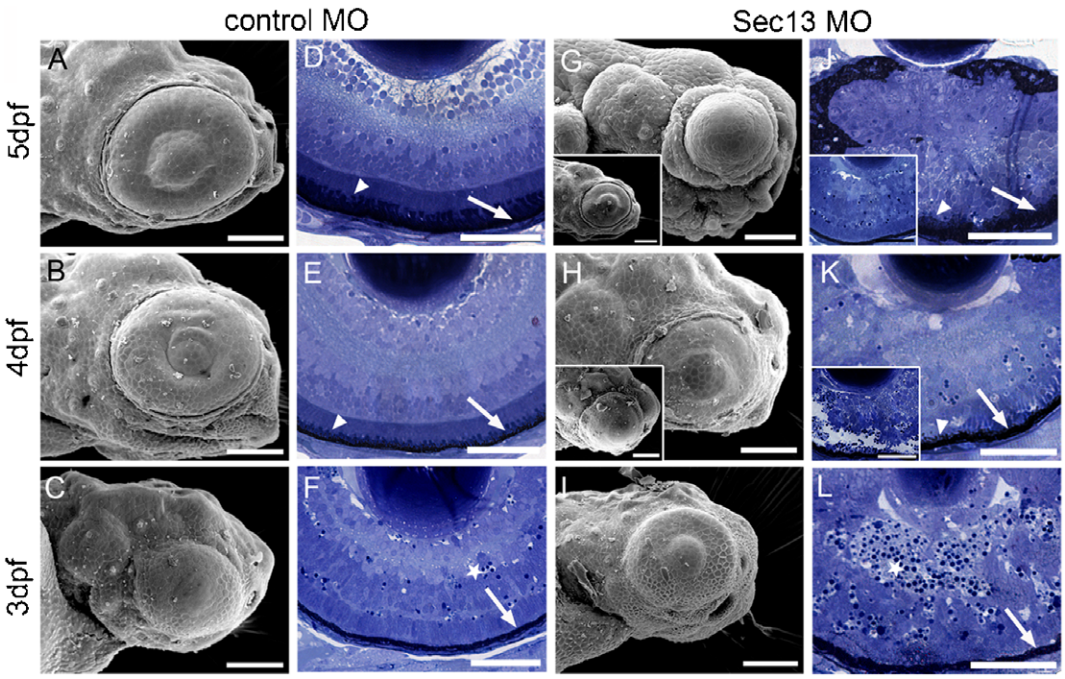

Fig. 1. Sec13 morphant phenotype. SEM of control (**A–C**) and Sec13 MO littermates (**G–I**). Scale bars: 100 µm. Toluidine Blue-stained 1 µm transversal sections of control (**D–F**) and Sec13 MO (**J–L**) from a comparable medial level. Scale bars: 50 µm. Insets in G,J,H,K show the other, less representative end of the phenotypic spectrum for 4 and 5 dpf, respectively. Arrows: RPE; arrowheads: outer segments of photoreceptors; stars: pyknotic nuclei/cell debris.

The histological phenotype was again more variable at 5 dpf (compare Fig. 1J and inset). Outer segments and discernible photoreceptors were lacking even in morphant eyes with a mild phenotype (Fig. 1J, inset), indicating that photoreceptor differentiation was not just delayed but greatly perturbed. Based on these results, photoreceptors and RPE were the most affected cell types in Sec13 deficiency.

Reduced cell proliferation and increased cell death in Sec13 morphant eyes

To gain further information about the onset of defects in retinal lamination, Sec13 morphant and control eyes were investigated at 2 dpf, prior to the morphological appearance of phenotypic changes. No apparent size difference was evident comparing histological sections of control and Sec13-depleted embryos (Fig. 2A,B), although the number of nuclei and mitotic profiles appeared reduced in morphant embryos (Fig. 2A,B, compare arrowheads). The overall number of proliferating cells was indeed smaller in Sec13 morphants (compare Fig. 2C,D) when phosphorylated histone 3 (pH 3) was labelled. To quantify the reduction in proliferation, 3 embryos each of Sec13 and control morphants were serially sectioned through the entire eyes and pH 3-positive cells were counted. 582±113 pH 3-positive nuclei were obtained from control eyes *versus* 174±40 cells in G2/M-phase in Sec13-depleted eyes. Not only was overall proliferation reduced but proliferating cells were additionally mispositioned in Sec13 morphant retinas. To determine the localisation of proliferating cells within the eye, pH 3-positive cells were scored by position in the retina and percentages of the total number of dividing cells were compared between control and Sec13 morphant samples (Fig. 2E). The ciliary marginal zone (CMZ) forms a ring around the lens and constitutes a stem cell area where progenitor cells divide to contribute to the expansion of the retina. The number of cells in G2/M-phase in the CMZ was significantly lower in Sec13 morphants (Fig. 2E). The rate of proliferation in adjacent apical positions was also significantly lower in Sec13-depleted embryos. Interestingly, the number of ectopically, basally dividing cells was much higher in Sec13 morphant eyes compared to controls. In contrast, no difference could be detected in the RPE.

In order to quantify cell death, live embryos were incubated with Acridine Orange (AO, Fig. 2F,G). AO labels structural changes in the DNA of damaged cells (Söderström et al., 1977). There was a significant increase in AO positive cells in Sec13 morphant eyes (Fig. 2H) when the average number of putatively non-phenotypic embryos (Fig. 2H, dotted oval) was excluded from the quantification. Increased cell death due to p53 activation can occur as a non-specific side effect of morpholino injections (Robu et al., 2007) and hence, could have contributed to the small eye phenotype. We therefore co-injected p53 morpholino oligonucleotides to block p53-dependent apoptosis and assessed the phenotype at 3 dpf when the highest level of cell death was detected (Fig. 2I–L). Co-injection of p53 oligonucleotides ameliorated the external appearance and size reduction of eyes of morphant embryos (compare Fig. 2I,J) but only marginally rescued kinked fins. Retinal lamination and photoreceptor development improved to some extent by inhibiting p53-driven apoptosis, but were not fully restored (compare Fig. 2K,L). We concluded that defects in retinal lamination and photoreceptor differentiation were not a mere consequence of p53-driven cell death. To verify the observed phenotype following Sec13 morpholino injection, we co-injected zebrafish Sec13 mRNA lacking the 5′UTR together with antisense morpholino oligonucleotides which targeted a sequence before the start

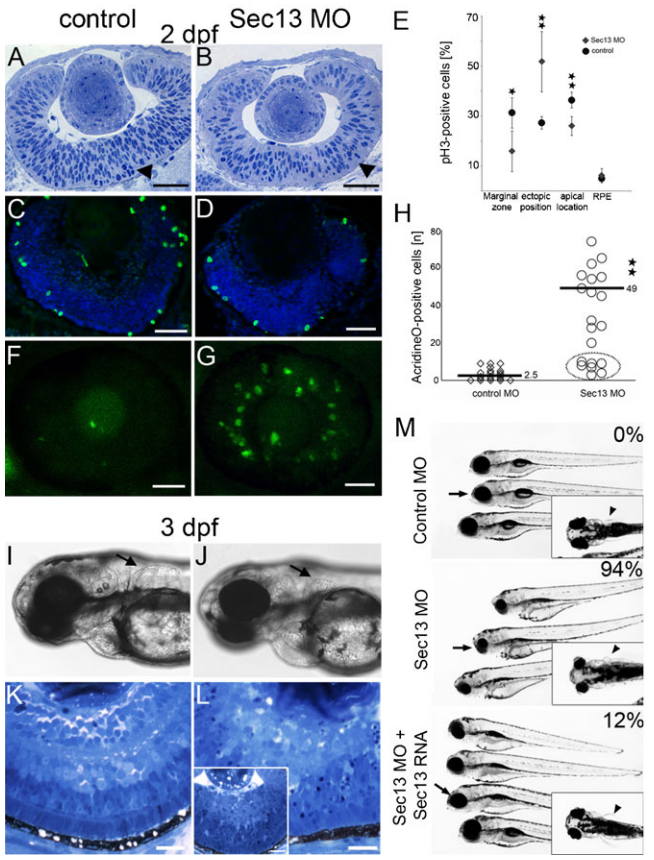

Fig. 2. Rescue of Sec13 knock-down phenotype. Toluidine Blue staining of 1 µm transversal sections of control (**A**) and Sec13 MO (**B**). pH 3 immunostaining on 10 µm sections of control (**C**) and Sec13 MO (**D**). Quantification of pH 3-positive cells (**E**). 582±113 pH 3-positive nuclei were obtained from control morphant eyes *versus* 174±40 cells in G2/M-phase in Sec13-depleted eyes. AO staining of control (**F**) and Sec13MO (**G**). Dotted oval: injected embryos without phenotype therefore excluded from mean values (**H**). Co-injection of p53 MO with control (**I**,**K**) or Sec13 MO (**J**,**L**). Live images, representative of 40 embryos each (I,J), and Toluidine Blue stained resin sections (J,K). Rescue experiment (**M**). Embryonic phenotype was scored according to eye (arrows) and fin phenotype (arrowheads, insets). Number of phenotypic embryos is given as percentage (M, top right). Quantification from at least 60 embryos each from 3 independent experiments. Scale bars: 20 µm.

codon (Fig. 2M). Co-injection of Sec13 mRNA in more than 60 embryos neutralised the effects of Sec13 knock-down at all concentrations higher than 20 pg in 82% of the injected embryos. Eye size and head shape were restored as, in this case, was the fin phenotype (Fig. 2M, compare middle and bottom panel). These data showed that Sec13 depletion in zebrafish embryos predominantly affected photoreceptor development and retinal lamination irrespective of p53-dependent apoptosis.

Sec13 depletion primarily affects photoreceptor development

To determine whether all retinal cell types were equally disrupted by Sec13 depletion and to further assess the phenotype of the inner retina, the presence and distribution of marker antigens for cell types were investigated. All sections in Fig. 3 were counterstained for nuclei (blue) and actin (red) to give an indication of the relative localisation within the retina. At 3 dpf (Fig. 3A), cones were differentiated, showed the typical elongated cell shape and were without exception lined up as a monolayer adjacent to the RPE in controls. Rod photoreceptor cells develop slightly later than cones and are less numerous in zebrafish; they also exclusively adjoined the RPE in control embryos (Fig. 3B). Amacrine and ganglion cells enclosed the IPL (inner plexiform layer) with amacrine cells exclusively occupying the basal half of the ONL (outer plexiform layer, Fig. 3C), and the optic nerve was clearly identifiable in control samples (Fig. 3D). Mueller glia cells are the last cell type to differentiate in zebrafish retinas; they were detectable but not yet abundant at 3 dpf in controls (Fig. 3E). In contrast, none of the cell types were comparably numerous in Sec13-depleted retinas (Fig. 3F,G) at 3 dpf. Rods had not developed at all (Fig. 3G) and cones were severely underrepresented (Fig. 3F), as were amacrine and ganglion cells and consequently, the optic nerve (Fig. 3H, Fig. 3I and inset). In most cases, cells that had at least acquired a defined cell fate were detected in ectopic locations reflecting the lack of retinal lamination. Mueller glia cells were also reduced in number but comparatively less affected than other cell types at 3 dpf. At 4 dpf, control retinas had advanced in development (Fig. 3K–O). Notably, Mueller glia cells and rods were more numerous (Fig. 3L,O). In Sec13 morphant retinas, on the other hand, all cell types were still less abundant (Fig. 3P–T) although the number of cones (Fig. 3P) and rods (Fig. 3Q) had risen relative to younger stages. Even though retinal development had recovered to some extent at 4 dpf (compare with Fig. 1K), none of the cell types were confined to the correct location within the retina in Sec13 morphant embryos. The absence of retinal lamination was also obvious from staining for actin (Fig. 3P–T, shown in red) and disorientation of Mueller glia cells (Fig. 3T, shown in green) suggesting that polarity within the retina was not properly established. Thus, retinal organisation was severely disturbed in Sec13 morphant eyes and encompassed all cell types. Importantly, rods and cones were more affected than other neuronal cell types, both in number and position within the retina. This again underlined that photoreceptor development was more impaired by the lack of full Sec13 function.

Opsin trafficking is perturbed in Sec13 morphants

It has been shown that undifferentiated, malfunctioning, or absent photoreceptors can negatively impact on an otherwise intact RPE (Strauss, 2005; Tsujikawa and Malicki, 2004) as well as lead to alterations in retinal lamination (Ray et al., 2010). To explore this possibility and get a better understanding of their state of differentiation, we first examined cones by confocal microscopy at 4 dpf. In control embryos, cones were lined up as a single layer of elongated cells directly adjacent to the RPE as visualised by labelling their inner segments (Fig. 4A). The apical side of control cones was equally defined and sealed in by an actin-rich OPL (Fig. 4A, see phalloidin stain in red). As previously shown, a number of cells in Sec13 morphants did acquire a photoreceptor cell fate, although they did not form a monolayer and were instead scattered around the retina (Fig. 4C). Among these cells, there were hardly any polarised, elongated photoreceptors identifiable. Rather, they presented with a rounded shape and very little cytoplasm. Later stages of cone differentiation are characterised by enrichment of opsin in their outer segments. Opsin represents the main transport burden for photoreceptors. The outer segments of control photoreceptors were labelled intensely with opsin as expected by 4 dpf (Fig. 4B). Although most photoreceptors in Sec13 morphants also expressed opsin demonstrating that they attempted to differentiate (Fig. 4D),

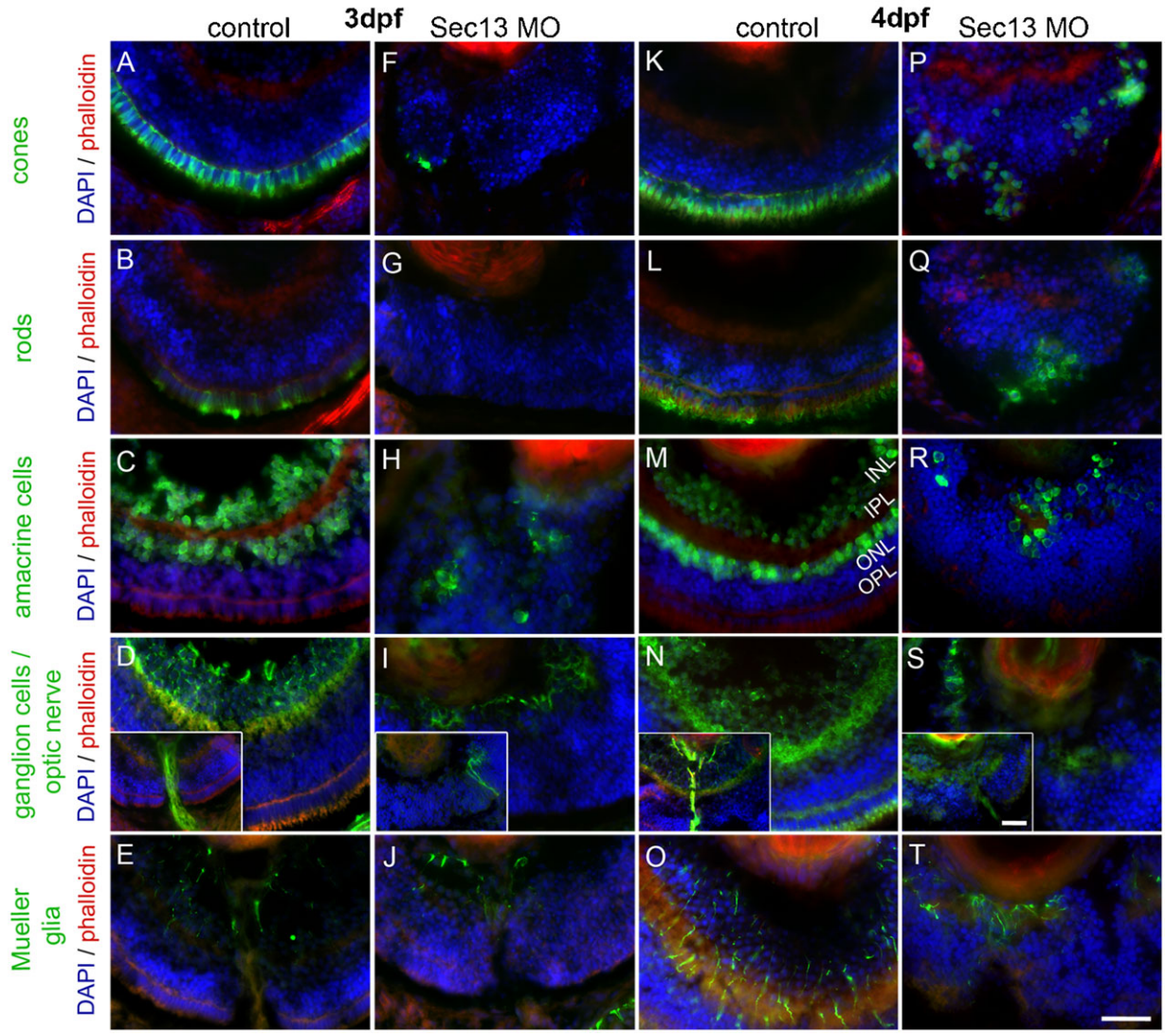

Fig. 3. Cellular identities in embryonic Sec13 knock-down eyes (A–T). Immunohistochemistry of medial transversal sections. The following antibodies were used to identify cell types: zpr-1 (cones), zpr-3 (rods), HuC/D (amacrine and ganglion cells), zn-5 (ganglion cells incl. axons) and zrf-1 (Mueller glia). Insets in D,I,N,S: optic nerve/axons of ganglion cells. INL: inner nuclear layer; IPL: inner plexiform layer; ONL: outer nuclear layer; OPL: outer plexiform layer. Scale bars: 20 µm.

opsin appeared to be confined to spots and patches (Fig. 4D, arrowhead). This suggested that opsin may have accumulated near the plasma membrane and/or in intracellular compartments and its intracellular transport may have been impaired. Accumulation of cargo proteins along the secretory pathway often results in dilation of respective intracellular compartments. To compare photoreceptors on an ultrastructural level, examples of weaker knock-down with discernible elements of outer segments were chosen to ascertain cell identity (Fig. 4E,F, stars). As expected, dilated membranous structures could be verified in Sec13-depleted photoreceptors by TEM (compare Fig. 4E,F). Whereas Golgi and ER were easily detectable by appearance in control photoreceptors (Fig. 4E, inset for second example), neither compartment was morphologically identifiable in Sec13-suppressed photoreceptors (Fig. 4F, inset for second example). Instead, all vesicular and tubular structures were expanded and budding profiles that appeared to be coated were frequently found (Fig. 4F, arrowheads). These data corroborated our previous findings that Sec13 depletion resulted in dilated ER with budding profiles (Townley et al., 2008) and supported the hypothesis that opsin may in fact have accumulated along the early secretory pathway.

In order to assess whether these dilated compartments were actually enriched with opsin, immunogold labelling was performed. Opsin specifically localised to the tight membrane stacks of cone outer segments in control photoreceptors and was rarely found in the inner segment (Fig. 4G, star; data not shown). In Sec13-suppressed photoreceptors on the other hand, opsin was mostly detected in dilated vesicular compartments near the cell surface (Fig. 4H, arrowheads, inset for second example), and in enlarged membrane-bound intracellular compartments (Fig. 4H, inset, star). These data demonstrated that pre-Golgi trafficking of opsin was compromised in Sec13 morphant eyes. Other studies have illustrated that accumulation of opsin in the ER and the resulting ER stress can lead to photoreceptor degeneration and early absence (Deretic and Wang, 2012; Frederick et al., 2001;

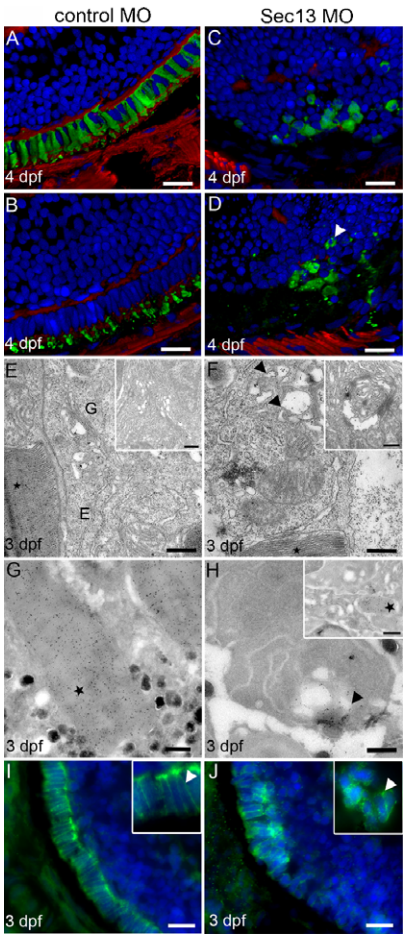

Fig. 4. Photoreceptor development and opsin transport in Sec13 morphant eyes. 3D opacity view of control (**A**,**B**) and Sec13 MO (**C**,**D**) stained for cones (zpr-1, A,C) and opsin (B,D) (green), phalloidin (red) and DAPI (blue). Arrowhead: dotted opsin localisation in Sec13 MO. Scale bars: 10 µm. TEM of control (**E**) and Sec13 MO (**F**), see insets for additional examples. Stars: outer segments; E: ER; G: Golgi; arrowheads: dilated ER and Golgi. Scale bars: 500 nm. Immunogold-labelling of opsin. Control (**G**) and Sec13MO (**H**). Arrowhead: accumulation of opsin in cell periphery. Stars: opsin label in outer segments. Scale bars: 500 nm. Immunolocalisation of syntaxin-3 in control (**I**) and Sec13 MO (**J**). Arrowheads: syntaxin-3 label at plasma membrane. Scale bars: 10 µm.

Tan et al., 2001) suggesting this could have been an underlying cause for the low number of photoreceptors in Sec13 morphants.

Since enrichment of rhodopsin in the ER was based on a deficiency in the trafficking machinery rather than a cargo-inherent property, we investigated the localisation of another membrane-bound protein to define whether the effect of Sec13 suppression may be general. Syntaxin-3A is confined to the plasma membrane of the inner segment of photoreceptors, and its correct position is necessary for rhodopsin transport and outer segment biogenesis (Baker et al., 2008; Chuang et al., 2007; Mazelova et al., 2009). In control photoreceptors, syntaxin-3A was found at the plasma membrane of the inner segment at 3 dpf as expected (Fig. 4I, and inset, arrowhead). Syntaxin-3A also correctly localised in Sec13-depleted photoreceptors (Fig. 4J) regardless of whether they had attempted to form an outer segment or not (Fig. 4J, inset, arrowhead). We have shown previously that Sec13 depletion differentially impaired transport of cargo proteins depending on their size and solubility (Townley et al., 2008). Here, both rhodopsin and syntaxin are insoluble and have approximately the same size (26 kD *versus* 40 kD) but transport was not equally affected. The amount of rhodopsin continuously trafficked to the outer segment is very likely to be higher than the amount of syntaxin-3A. This suggested that efficient assembly and stability of the outer coat was equally necessary for transport of large amounts of cargo as for the formation of large carriers. It has also been shown that rhodopsin follows a specialised transport route in separate vesicles, at least post-Golgi (Deretic and Papermaster, 1991), and this may differ between rods and cones (Karan et al., 2008). In addition, rhodopsin molecules oligomerise in at least the outer segment membrane. It is not yet clear whether and to what extent either aspect might also be relevant for ER-to-Golgi trafficking. Thus, although it was not possible to deduce from a comparison of just two cargo proteins that the defect induced by Sec13 was truly rhodopsin-specific, it could be concluded that transport was not generally impaired and an important requirement for outer segment biogenesis was in place. These data suggested that disrupted rhodopsin transport underlay the failure to develop outer segments, although they could not explain the reduction in number of photoreceptors from the onset and their mislocalisation within the retina.

Formation of Bruch's membrane and collagen secretion are impaired in Sec13 morphant eyes

Several studies have shown that a functional RPE supports retinal lamination as well as photoreceptor polarisation and differentiation (Bok and Hall, 1971; German et al., 2008; Hollyfield and Witkovsky, 1974; Jeffery, 1998; Krock et al., 2007; Longbottom et al., 2009; Marmorstein et al., 1998; Raymond and Jackson, 1995). The RPE in Sec13 morphant eyes appeared hypertrophic and could have been dysfunctional (compare with Figs 1, 3). Since we had shown previously that disruption of Sec13 function led to a greatly decreased transport of large cargo, namely procollagens, and collagen type IV is an integral part of the Bruch's membrane, we next investigated the presence and composition of the basal lamina. Abnormal establishment of the Bruch's membrane would result in a non-polarised RPE unable to assist retinal lamination and photoreceptor differentiation.

Fracture surfaces of control and Sec13 morphant eyes at 4 dpf were examined by SEM for a first gross morphological assessment (Fig. 5A,B). The elongated cell shapes of photoreceptors were easily discernible in control eyes (Fig. 5A, P) as was the nodular surface created by melanosomes of the RPE (Fig. 5A, RPE). The RPE in control eyes resided on a smooth extracellular layer overlying ocular muscle fibres (Fig. 5A, arrow). In Sec13-depleted eyes, the laminar structure of the retina was absent (Fig. 5B); likewise, the RPE appeared hypertrophic and did not show a similar nodular structure as in controls (Fig. 5B, RPE). A photoreceptor layer was not identifiable. A discrete basal lamina was also missing in Sec13 morphant eyes (Fig. 5B, inset for second example). However, the basal surface of the RPE, even though undulated, appeared smooth (Fig. 5B, arrow). All embryos examined here gave comparable results ($n>20$, several independent spawns).

In TEM images taken from the medial part of the eyes, a distinct electron-dense sheet was clearly visible in control eyes (Fig. 5C, arrow). This was missing in Sec13 morphant eyes

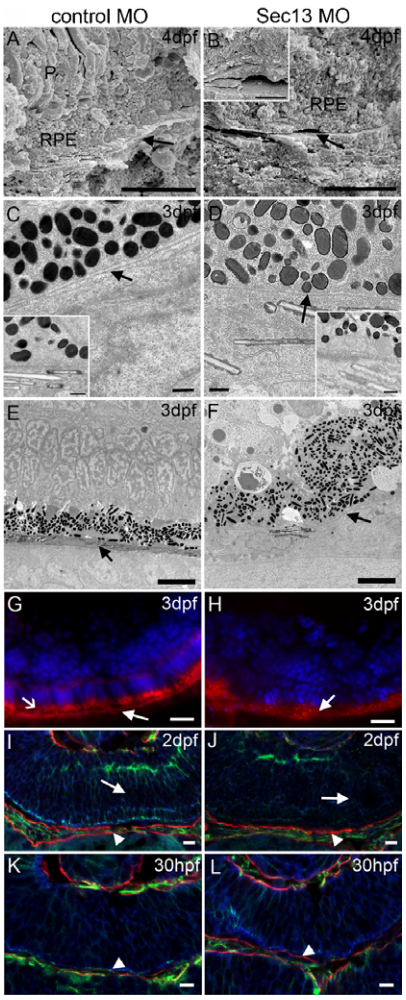

Fig. 5. Basal lamina/Bruch's membrane in Sec13 knock-down embryos. SEM of internal surfaces of control (**A**) and Sec13 MO (**B**, inset for second example) indicating Bruch's membrane (arrows). P: photoreceptor layer; RPE: retinal pigment epithelium. Scale bars: 10 µm. TEM of control (**C**) and Sec13 MO (**D**). Arrows: basal lamina. Insets: second examples. Scale bars: 500 nm. Tannic acid/uranyl acetate stain of control (**E**) and Sec13 MO (**F**). Representative for 2 embryos each. Arrows: collagen-rich layer. Scale bars: 5 µm. Immunohistochemical staining for collagen IV of control (**G**) and Sec13 MO (**H**) albino fish. Arrows: collagen IV layer; open arrow: auto-fluorescence of outer segments. Scale bars: 10 µm. Immunohistochemical staining for laminin (green), actin (red, arrowheads) and β-catenin (blue) of control (**I**,**K**) and Sec13 MO (**J**,**L**). Arrows: disorganisation of retinal neuroepithelium shown by laminin and β-catenin labelling. Representative image of 12 embryos. Scale bars: 10 µm.

(Fig. 5D, arrow), supporting the SEM data. The differences were less apparent in pictures obtained from the peripheral regions of the eyecups (Fig. 5C,D, insets). Thus, TEMs also pointed towards a deficiency in Bruch's membrane deposition. To unequivocally confirm these observations we performed a combined staining with uranyl acetate and tannic acid, which enhances the contrast of elastin-rich elastic fibres in electron microscopy and also results in a moderately increased electron density of collagen (Haidar et al., 1992; Hayat, 2000). An electron-dense fibrous sheet was clearly identifiable in control eyes (Fig. 5E, arrow) at 3 dpf. However, an equivalent electron-dense layer was not present in any of the Sec13-depleted embryos (Fig. 5F, arrow) although the basal side of the RPE was again well defined. Therefore, even though attempts to form the Bruch's membrane occurred, there may have not been sufficient amounts of elastin or collagen in Sec13 morphant eyes to fully support the formation of a functional basal lamina.

As additional confirmation of a functional and polarised RPE, we analysed the distribution of components of the Bruch's membrane by immunofluorescence at 3 dpf. Collagen type IV formed a defined layer below the RPE in control eyes (Fig. 5G, arrow) whereas it was detected in a spotty pattern throughout the RPE in Sec13 knock-down embryos (Fig. 5H, arrow). In light of our previous studies (Townley et al., 2008), showing a trafficking defect of collagens in Sec13-depleted fibroblasts the collagen IV staining in the eye could be interpreted to represent collagen accumulation within the cells. Taken together, these data suggested that collagen IV was reduced in the extracellular space, leaving open the possibility that the RPE might not be polarised and consequently not functional, although there were indications that some kind of basal lamina was still present in Sec13-depleted eyes (see also Fig. 5D, inset).

To test whether the RPE in Sec13 morphant embryos was polarised, we investigated β-catenin localisation. No significant difference between control and Sec13 morphant eyes could be detected at 2 dpf (Fig. 5I,J, compare arrowheads). At this stage, the retinal neuroepithelium was already disorganised (Fig. 5I,J, compare arrows) suggesting that retinal disorganisation was initially independent of RPE polarisation. Earlier, at 30 hpf, RPE and retina were also indistinguishable between control and Sec13 MO eyes (compare Fig. 5K,L). Thus, the RPE could have supported retinal lamination and photoreceptor differentiation irrespective of its later hypertrophic appearance.

Cell autonomy of trafficking defects in Sec13 morphant eyes

We demonstrated transport defects in photoreceptors and RPE but it was unclear whether faulty retinal development was due to defects in RPE organisation or photoreceptor differentiation or whether both aspects were interdependently causing the phenotype. In order to test whether Sec13 function was required cell-autonomously or non-autonomously, we generated chimeric zebrafish larvae by blastomere transplantation (Fig. 6). Blastomeres from donor embryos were injected into the presumptive eye region (Kimmel et al., 1990) of host embryos. The phenotypic outcome was evaluated morphologically by altered cell shape and fluorescence labelling for photoreceptor identity. Lamination defects were defined by presence of nuclei in the IPL (Fig. 6E). For instance, if Sec13 functions cell-autonomously in the retina, we would anticipate that clones in the RPE alone would not have an effect on photoreceptor development while clones in photoreceptors would perturb their differentiation.

Based on our previous results we first investigated chimeric embryos at 4 dpf. Eye development was externally indistinguishable from control embryos when Sec13 deficient cells were transplanted into wild-type hosts (Fig. 6A). In all transplanted retinas, dextran-fluorescein was detected as spots reminiscent of the condensed cells and pyknotic nuclei seen in histology (compare with Fig. 1K), suggesting that Sec13-depleted cells could not be rescued by surrounding wild-type cells, and have undergone cell death by 4 dpf. Conversely, control cells transplanted into a Sec13 deficient background frequently appeared to have outcompeted Sec13-depleted host cells (Fig. 6B) resulting in overly large transplants encompassing

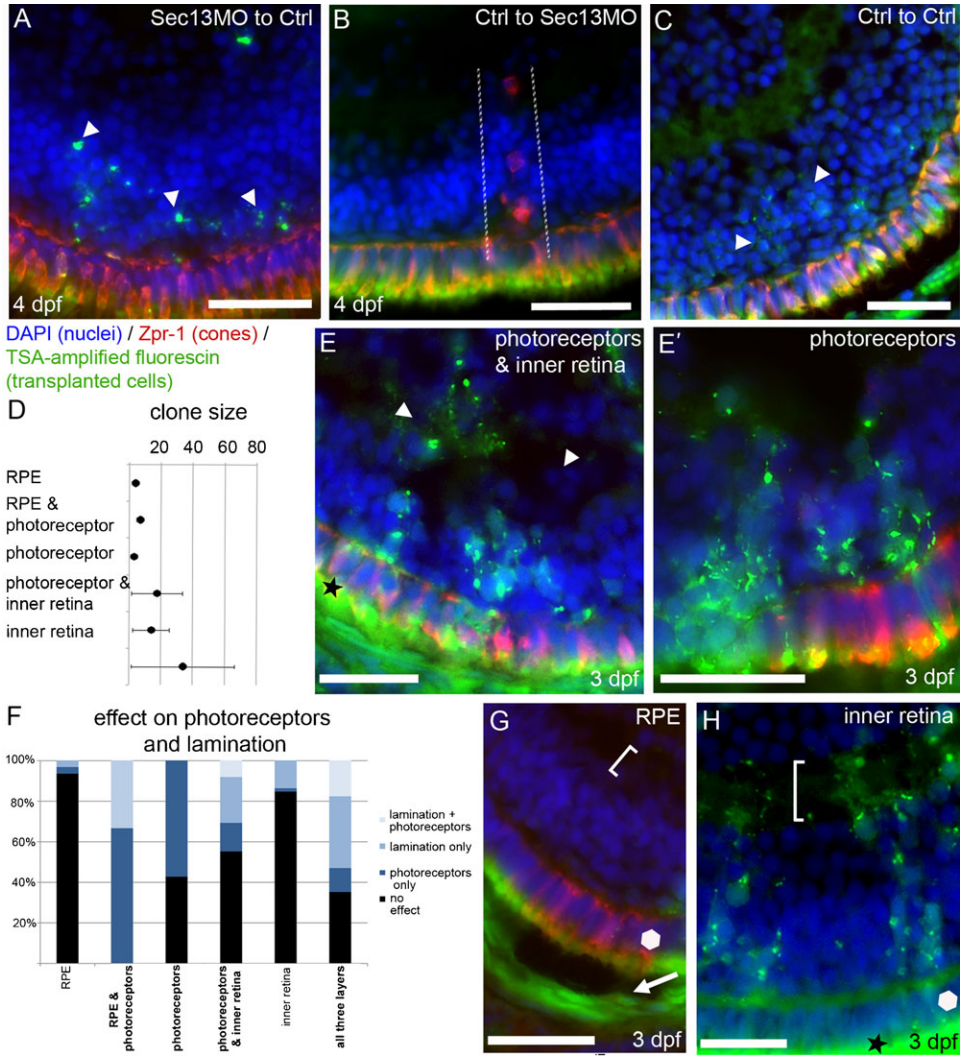

Fig. 6. Cell autonomous effect of Sec13 depletion. Dextran-fluorescin-labelled donor blastomeres were transplanted into host blastulas as indicated. Dextran-fluorescin was detected by TSA amplification (green), cones were identified by zpr-1 labelling (red) and nuclei were stained with DAPI (blue). Examples of blastomere transplants from/to LonAB embryos at 4 dpf (**A–C**). Arrowheads (A): apoptotic morphant cells. Dotted lines (B): photoreceptor cells derived from the Sec13 MO host. Arrowheads (C): transplanted control cells. Blastomere transplantation into albino wild-type embryos (**D–H**). Sec13 morphant transplants were fluorescin-positive (green) or identified by presence of melanosomes (black cell layer, arrow in G). Graphical depiction (D) of the average number of transplanted blastomeres in each clone (black dots). Phenotypic transplants scored for impact on photoreceptors and/or lamination or no effect shown as fractions of 100% with respect to the number of clones in each category (F). Layers including photoreceptors (bold font) showed more effect. Photoreceptors and lamination: light blue, lamination: medium blue, photoreceptors: dark blue, no effect: black. Examples of transplants (green and/or pigmented) as indicated (E,E′,G,H). Photoreceptors (Zpr-1) in red and nuclei in blue. Arrow: Sec13 derived RPE cells; arrowheads: defects in retinal lamination; brackets: no effect on lamination; polygons: no effect on photoreceptors; star: autofluorescence of outer segments. Scale bars: 20 μm.

nearly the whole retina. Transplanting control cells into a wild-type host never resulted in a phenotype (Fig. 6C). Taken together, these results pointed towards a cell autonomous requirement for Sec13 since neither the lamination defect nor the propensity to cell death of Sec13 morphant cells could be rescued by surrounding control cells.

Since out-competing control cells were not informative to test the initial hypothesis, we screened the phenotypic outcome at 3 dpf to avoid losing Sec 13 deficient clones (Fig. 6D–H). Sec13-depleted blastomeres were transplanted into wild-type albino embryos and selected for successful transplantation at 1 dpf. Only embryos with fluorescein-labelled cells in the eye region were retained for further evaluation. This approach also bypassed autofluorescence derived from RPE pigmentation that may have obscured fluorescein-labelled cells. At 3 dpf, 26% of the embryos had entirely lost their transplants specifically in the eyes (10 of 38) underlining previous results of Sec13-suppressed blastomeres undergoing cell death. A further 26% (10 of 38 embryos) showed no sign of pigmentation around the eyes at 3 dpf; the RPE was therefore absent in these clones. Altogether, 173 retinal clones from 29 embryos were quantified. The average clone size varied substantially (Fig. 6D) but generally correlated with the thickness and number of retinal layers. Interestingly, the number of transplants in each category did not follow this pattern. Transplants in ‘RPE & photoreceptor’ (4) or ‘photoreceptor’ (6) were more rare than clones in ‘RPE’ (36). This again suggested that Sec13-depleted photoreceptors were more prone to undergo cell death or that Sec13-depleted cells were more likely to be excluded from the photoreceptor layer.

To quantify the phenotypic outcomes, transplants were grouped in ‘no effect’, ‘effect on photoreceptors’, ‘lamination only’ and ‘lamination and photoreceptors’ (Fig. 6F). Respective phenotypes in each category were shown as fractions of 100%. The quantification suggested that a trafficking defect in the RPE alone was not the primary cause for the morphant phenotype of the eyes (Fig. 6F,G). Clones in the inner retina alone also barely had any phenotypic effect (Fig. 6F,H). In both cases, lamination was mainly normal with correctly aligned nuclei (Fig. 6G,H, brackets) and photoreceptor cells were not impaired (Fig. 6G,H, polygons). Non-elongated cell shape of photoreceptors was nearly only found if the photoreceptor layer was included in the clone (Fig. 6E,E′,F). Comparing the autofluorescence of outer segments, Sec13 deficient cells in the photoreceptor layer either did not acquire photoreceptor identity at all (Fig. 6E′) or may have not developed outer segments (Fig. 6E) unlike the photoreceptors in ‘RPE only’ or ‘inner retina’ transplants

(Fig. 6G,H). Since outer segments with membrane discs can only develop if opsin is transported correctly we assumed that there was no trafficking defect in these cases. Altered laminar structure of the retina mostly required the inner retina to be part of the clone (Fig. 6E). Overall our data suggest that Sec13 is required cell-autonomously, specifically in photoreceptors.

Discussion

We have shown here that depletion of Sec13 in zebrafish leads to small eyes with a disorganised retinal neuroepithelium. Consistent with our previous results (Townley et al., 2008), collagen transport from the RPE was compromised. These data therefore support our previous model that highly efficient assembly of the outer COPII coat is required for trafficking of large cargo.

The phenotype of Sec13 depletion described here is comparable to the phenotype of a recently published Sec13 mutant zebrafish (Niu et al., 2012), and both become apparent after 2 dpf. Morphant and mutant both show small eyes with a protruding lens. The onset of phenotypic changes in Sec13 knock-down and Sec13 mutant zebrafish could be caused by maternally supplied mRNA or protein since it has been shown that both are present in the early embryo (Niu et al., 2012). The morpholino oligonucleotides used in our study recognise a sequence within the open reading frame and hence should block translation of maternal as well as zygotic mRNA. Therefore, the relatively late appearance of the eye phenotype was likely due to maternally supplied protein or a negligible role for Sec13 function up to this age. It has been suggested that maternally supplied Sec13 mRNA and/or protein may also have been the reason for ongoing secretion such as laminin until 5 dpf in Sec13 mutant zebrafish; however, 5 days would seem a rather long half-life for either. In our study, we interpret the variability observed at 5 dpf not as a sign of dilution of maternal protein but of morpholinos instead. It is known that the concentration of morpholino oligonucleotides per cell decreases with ongoing cell division and the knock-down effect may therefore diverge between tissues as development proceeds (Bill et al., 2009; Eisen and Smith, 2008; Sumanas and Larson, 2002).

From 2 dpf, when morphological changes become detectable in Sec13 morphants and mutants (Niu et al., 2012), there is a transition in retinal development where proliferation ceases centrally but continues in the marginal zone. Earlier in development, the undifferentiated neuroepithelium proliferates at a high rate, mostly on the apical side i.e. adjacent to the RPE. Reduced proliferation as well as increased cell death could lead to a delay in differentiation that in turn might impair the apico-basal integrity of the retinal neuroepithelium. Indeed, we found proliferation to be reduced and occurring ectopically as well as increased apoptosis in Sec13-depleted embryos. However, apico-basal polarity of the neuroepithelium was not affected at any stage investigated, even when the lamination defect was already visible. In addition, there was no difference in the number and location of proliferating cells at earlier stages (data not shown). This suggests that the observed lamination defect in Sec13 morphants is not caused by impaired proliferation or increased apoptosis. How the alteration of proliferation and apoptosis is mechanistically linked to Sec13 depletion was beyond the scope of this study and will require further detailed research.

Prior to neurogenesis, the neuroepithelium was not perturbed in Sec13 morphant zebrafish. Later in development, the number and distribution of differentiating retinal cell types across all layers were altered but not all cell types were equally affected. Retinal ganglion cells are the first to leave the cell cycle and differentiate just after 1 dpf (Schmitt and Dowling, 1994). They were reduced in number and disorganised in Sec13-depleted retinas when compared to control samples but they still differentiated roughly in the correct location and developed axons to generate attempts of an optic nerve. Amacrine and Müller glia cells were also fewer and mislocalised but since they differentiate after lamination is already established in zebrafish this might be a secondary effect to retinal disorganisation. Photoreceptors leave the cell cycle at around 2 dpf when the proliferation and cell death aspects of the phenotype first become detectable (Hu and Easter, 1999). Opsin expression starts between 2 dpf and 3 dpf (Tsujikawa and Malicki, 2004). The secretory load during photoreceptor differentiation and subsequent maintenance is very high; ~50,000 molecules of opsin need to be transported per minute (Besharse and Horst, 1990; Young, 1967). Rhodopsin is crucial for photoreceptor development and survival since mice lacking rhodopsin do not develop outer segments and photoreceptors degenerate (Humphries et al., 1997; Rosenfeld et al., 1992). We propose that the effect of Sec13 suppression in photoreceptors is most likely caused by a combination of effects. First, reduced proliferation results in fewer photoreceptors. As proliferation happens ectopically, photoreceptors differentiate in random positions. Second, defective opsin trafficking interferes with photoreceptor maturation and leads to apoptosis or incomplete differentiation.

Photoreceptor development and maintenance requires interaction with an intact RPE (Bok and Hall, 1971; Hollyfield and Witkovsky, 1974; Jeffery, 1998; Marmorstein et al., 1998). Contact with the RPE is necessary for opsin expression and outer segment development; photoreceptors only continue to differentiate *in vitro* when seeded on top of RPE cells (German et al., 2008). We have shown that the RPE of Sec13 morphants was hypertrophic and disorganised; furthermore our data suggest that collagen transport was impaired following Sec13 depletion. Collagen Type 4 is the major constituent of the basement membrane of the RPE. Basement membranes determine the polarity of cells and organisation of tissues. Mutations in collagen type 4 result in retinal dysgenesis or degeneration (Bai et al., 2009). Thus, a non-polarised RPE could have partially explained the photoreceptor phenotype. However, RPE hypertrophy only became apparent after disruption of retinal lamination was already obvious. Moreover, we never saw any indication of lack of polarity of the RPE. Hence, even though the RPE could be dysfunctional later, this is unlikely to be causative for the early phenotype. Instead, the RPE phenotype could be a secondary consequence of absent photoreceptor cells, as the RPE frequently appears thicker and disorganised in blind fish (Cerveny et al., 2010; Malicki et al., 1996). Polarity of RPE and photoreceptors is interdependently established (Bok, 1993; Marmorstein, 2001; Marmorstein et al., 1998). Our blastomere transplantation data, however, suggest that Sec13 knock-down may act cell-autonomously throughout the retina.

Taken together, we have clearly demonstrated trafficking defects in the RPE and in photoreceptors following depletion of Sec13. The incomplete differentiation of elongated photoreceptors was most likely resulting from deficient rhodopsin transport. Rhodopsin is an average sized protein of

40 kD. Therefore, we suggest an addendum to the prevailing hypothesis of Sec13 function. Sec13 and the outer COPII coat are not only indispensable for transport of large/unusual cargo but also for transport of unusually large amounts of cargo, at least in the context of photoreceptor differentiation and maintenance. The consequent degeneration of photoreceptors indirectly impacts on the formation of the whole eye but cannot account for the early defect in retinal lamination. Whether disorganisation of the retina is directly caused by a trafficking defect and in which cell type or even by Sec13 function at the nuclear pore (Siniossoglou et al., 1996) will have to be determined in future studies.

Materials and Methods

Danio rerio husbandry and morpholino oligonucleotide microinjection

Zebrafish (LonAB strain) were raised and maintained as described previously (Townley et al., 2008; Westerfield, 2000). Two non-overlapping, translation-blocking morpholino oligonucleotides (MO) targeting *D. rerio* Sec13 (BC153483.1) were designed and synthesised by GeneTools LLC (Philomath, OR). Sequences of the oligonucleotides and confirmation of knock-down as well as expression levels of Sec31 and α-tubulin were published previously (Townley et al., 2008). Only results of MO2 are shown here. Morpholino and standard control oligonucleotides (GeneTools) were injected at the 1-to-4-cell stage (approx. 1 nl, 10–20 pg). Injected embryos were anaesthetised and processed for the respective experiments. To inhibit p53 function, 1-to-4-cell stage LonAB embryos were co-injected with equal amounts of p53 (GeneTools) and Sec13 MO.

Blastomere transplantation and rescue

LonAB embryos were injected at the 1-cell stage with Sec13 morpholino oligonucleotides (10–20 pg per embryo) and dextran-fluorescein (40 kMW, Molecular Probes) in equal amounts. About 40 Sec13MO-dextran labelled cells were transplanted into early-gastrula-staged LonAB or Albino hosts in the region fated to become the eye (Cavodeassi et al., 2005; Woo and Fraser, 1995). A subset of donor embryos was allowed to grow until 3 dpf to determine the ratio of morphants to non-phenotypic siblings. The outcome was assessed by TSA amplifying the dextran-fluorescein signal and labelling for photoreceptors as well as counterstaining for nuclei. For rescue experiments, zebrafish Sec13 (IMAGE clone 6792353 (BC054585)) was cloned into pCS2+. Capped Sec13 mRNA was prepared using a mMessage mMachine RNA Synthesis Kit (Ambion) according to the manufacturer's instructions. Sec13 mRNAs were co-injected with Sec13 MO at concentrations between 10 and 80 pg into 1-cell stage embryos. Embryos were raised until 3 dpf and imaged directly or processed for histology.

Immunohistochemistry

LonAB or Albino embryos were fixed in 3.5% paraformaldehyde in PBS for 2 hours on ice. Specimens were washed in PBS and cryo-protected in 30% sucrose overnight at 4℃. After embedding in OCT (Jung Histoservice) samples were stored at −80℃ before cutting 10–14 µm sections (20 µm for zfr-1, Leica CM3000). Sections were quenched with 50 mM glycine in PBS, permeabilised with 0.1% Triton X-100 and blocked with 5% normal donkey serum (NDS) for 1 hour. Primary antibodies were diluted in 2.5% NDS and incubated for 1 hour: opsin (1:1000, Sigma), HuC/D (1:300, Molecular Probes), zpr-1 (1:100, zebrafish international resource centre ZIRC), zrf-1 (1:100, ZIRC), zpr-3 (1:100, ZIRC), zn-5 (1:10, ZIRC), collagen IV (1:50, Fisher Scientific), phospho-H3 (1:1000, Upstate Biotechnology), β-catenin (1:200, Sigma) and syntaxin-3A (1:100, gift from A. Peden, Cambridge). Alexa568-conjugated phalloidin (1:200, Molecular Probes) and Alexa488 donkey-α-mouse (1:250, Jackson Laboratories) were incubated for 1 hour in the dark. Nuclei were counterstained with DAPI. Images were taken with an Olympus IX71microscope and a Coolsnap HQ2 camera (Photometrics) and processed with Adobe Photoshop CS4. Immunostaining for laminin (1:100, Sigma–Aldrich), γ-tubulin (1:400, Sigma–Aldrich) and phosphor-H3n (1:1000, Upstate Biotechnology) at 30 hpf and 48 hpf was performed as described previously (Cerveny et al., 2010). All experiments were done in triplicate.

Cell death and proliferation

Serial sections of 6 entire eyes for each condition were stained for pH 3. Statistical significance of mean values was calculated with Student's *t*-test. Live embryos were stained with AO (1 µg/ml) to assess cell death. More than 20 embryos for each condition were anaesthetised and imaged immediately. Mean values of AO-positive cells were compared by Student's *t*-test.

SEM

1 to 5 dpf zebrafish were fixed in 2.5% glutaraldehyde (GA)/0.1 M cacodylate, then post-fixed in 1% OsO_4 in cacodylate for 1 hour, dehydrated in graded ethanol, and critical-point dried. For imaging internal surfaces, specimens were fixed with 2% OsO_4 for 2 hours before sputter coating. All specimens were sputter-coated with gold (Edwards Sputter Coater) and viewed on a FEI Quanta4000 SEM. At least 20 embryos each were used in 3 independent experiments.

TEM and histology

Control and Sec13 MO zebrafish were fixed in 5% GA/0.05 M Cacodylate/1% Paraformaldehyde (PFA)/1% Sucrose/1 mM $MgCl_2$ for 2 hours. Samples were post-fixed in 1% OsO_4 and dehydrated. Specimens were infiltrated with Epon and 50 nm sections were contrasted with uranyl acetate and lead citrate and analysed with a FEI Tecnai12 Biotwin/4K EAGLE CCD camera. To further enhance contrast of elastin and collagen, specimens were embedded in LR White resin and counterstained with a mixture of tannic acid and uranyl acetate (Haidar et al., 1992). For histology, 1 µm Epon sections of fish from the same anterior–posterior region were counterstained with Toluidine Blue and imaged on a Zeiss Axioplan 2 microscope with a Qimaging digital camera. All TEM and histology images represent examples from 3 independent experiments.

Immunogold staining

Zebrafish were fixed in 4% PFA/01% GA for 3 hours, embedded in 12% Gelatine and infiltrated with 2.3 M sucrose overnight. 90 µm sections were blocked with 0.1% acetylated BSA (Aurion, Netherlands) and incubated with α-opsin antibody (1:100, Sigma–Aldrich) and secondary antibody (6 nm gold, Aurion) for 1 hour each.

Acknowledgements

The authors thank William Harris for discussion in the early stages of the project, Paul Martin for ongoing support of the zebrafish work in Bristol and Brooke Morriswood for critical reading of the manuscript. This work was supported by the BBSRC (BB/H008462/1 to F.C. and E019633 to K.S. and D.J.S.), the MRC (F.C.) and the Wellcome Trust (WT089227/Z/09/Z to F.C. and WT077988/Z05/Z to Y.F.).

Competing Interests

The authors have no competing interests to declare.

References

Aridor, M. and Hannan, L. A. (2000). Traffic jam: a compendium of human diseases that affect intracellular transport processes. *Traffic* **1**, 836-851.

Aridor, M. and Hannan, L. A. (2002). Traffic jams II: an update of diseases of intracellular transport. *Traffic* **3**, 781-790.

Aridor, M., Bannykh, S. I., Rowe, T. and Balch, W. E. (1999). Cargo can modulate COPII vesicle formation from the endoplasmic reticulum. *J. Biol. Chem.* **274**, 4389-4399.

Bai, X., Dilworth, D. J., Weng, Y. C. and Gould, D. B. (2009). Developmental distribution of collagen IV isoforms and relevance to ocular diseases. *Matrix Biol.* **28**, 194-201.

Baker, S. A., Haeri, M., Yoo, P., Gospe, S. M., 3rd, Skiba, N. P., Knox, B. E. and Arshavsky, V. Y. (2008). The outer segment serves as a default destination for the trafficking of membrane proteins in photoreceptors. *J. Cell Biol.* **183**, 485-498.

Barlowe, C., Orci, L., Yeung, T., Hosobuchi, M., Hamamoto, S., Salama, N., Rexach, M. F., Ravazzola, M., Amherdt, M. and Schekman, R. (1994). COPII: a membrane coat formed by Sec proteins that drive vesicle budding from the endoplasmic reticulum. *Cell* **77**, 895-907.

Besharse, J. C. and Horst, C. J. (1990). The photoreceptor connecting cilium: a model for the transition zone. In *Ciliary And Flagellar Membranes* (ed. R. A. Bloodgood), pp. 389-417. New York: Plenum Press.

Bhattacharya, N., O Donnell, J. and Stagg, S. M. (2012). The structure of the Sec13/31 COPII cage bound to Sec23. *J. Mol. Biol.* **420**, 324-334.

Bi, X., Mancias, J. D. and Goldberg, J. (2007). Insights into COPII coat nucleation from the structure of Sec23·Sar1 complexed with the active fragment of Sec31. *Dev. Cell* **13**, 635-645.

Bill, B. R., Petzold, A. M., Clark, K. J., Schimmenti, L. A. and Ekker, S. C. (2009). A primer for morpholino use in zebrafish. *Zebrafish* **6**, 69-77.

Bok, D. (1993). The retinal pigment epithelium: a versatile partner in vision. *J. Cell Sci. Suppl.* **17**, 189-195.

Bok, D. and Hall, M. O. (1971). The role of the pigment epithelium in the etiology of inherited retinal dystrophy in the rat. *J. Cell Biol.* **49**, 664-682.

Boyadjiev, S. A., Fromme, J. C., Ben, J., Chong, S. S., Nauta, C., Hur, D. J., Zhang, G., Hamamoto, S., Schekman, R., Ravazzola, M. et al. (2006). Cranio-lenticulo-sutural dysplasia is caused by a *SEC23A* mutation leading to abnormal endoplasmic-reticulum-to-Golgi trafficking. *Nat. Genet.* **38**, 1192-1197.

Cavodeassi, F., Carreira-Barbosa, F., Young, R. M., Concha, M. L., Allende, M. L., Houart, C., Tada, M. and Wilson, S. W. (2005). Early stages of zebrafish eye formation require the coordinated activity of Wnt11, Fz5, and the Wnt/β-catenin pathway. *Neuron* **47**, 43-56.

Cerveny, K. L., Cavodeassi, F., Turner, K. J., de Jong-Curtain, T. A., Heath, J. K. and Wilson, S. W. (2010). The zebrafish *flotte lotte* mutant reveals that the local retinal environment promotes the differentiation of proliferating precursors emerging from their stem cell niche. *Development* **137**, 2107-2115.

Chuang, J. Z., Zhao, Y. and Sung, C. H. (2007). SARA-regulated vesicular targeting underlies formation of the light-sensing organelle in mammalian rods. *Cell* **130**, 535-547.

Deretic, D. (2006). A role for rhodopsin in a signal transduction cascade that regulates membrane trafficking and photoreceptor polarity. *Vision Res.* **46**, 4427-4433.

Deretic, D. and Papermaster, D. S. (1991). Polarized sorting of rhodopsin on post-Golgi membranes in frog retinal photoreceptor cells. *J. Cell Biol.* **113**, 1281-1293.

Deretic, D. and Wang, J. (2012). Molecular assemblies that control rhodopsin transport to the cilia. *Vision Res*. **75**, 5-10.

Eisen, J. S. and Smith, J. C. (2008). Controlling morpholino experiments: don't stop making antisense. *Development* **135**, 1735-1743.

Frederick, J. M., Krasnoperova, N. V., Hoffmann, K., Church-Kopish, J., Rüther, K., Howes, K., Lem, J. and Baehr, W. (2001). Mutant rhodopsin transgene expression on a null background. *Invest. Ophthalmol. Vis. Sci.* **42**, 826-833.

Fromme, J. C., Ravazzola, M., Hamamoto, S., Al-Balwi, M., Eyaid, W., Boyadjiev, S. A., Cosson, P., Schekman, R. and Orci, L. (2007). The genetic basis of a craniofacial disease provides insight into COPII coat assembly. *Dev. Cell* **13**, 623-634.

German, O. L., Buzzi, E., Rotstein, N. P., Rodríguez-Boulan, E. and Politi, L. E. (2008). Retinal pigment epithelial cells promote spatial reorganization and differentiation of retina photoreceptors. *J. Neurosci. Res.* **86**, 3503-3514.

Haidar, A., Ryder, T. A., Mobberley, M. A. and Wigglesworth, J. S. (1992). Two techniques for electron opaque staining of elastic fibres using tannic acid in fresh and formalin fixed tissue. *J. Clin. Pathol.* **45**, 633-635.

Hayat, M. A. (2000). *Principles And Techniques Of Electron Microscopy: Biological Applications*. Cambridge: Cambridge University Press.

Hollyfield, J. G. and Witkovsky, P. (1974). Pigmented retinal epithelium involvement in photoreceptor development and function. *J. Exp. Zool.* **189**, 357-377.

Hu, M. and Easter, S. S. (1999). Retinal neurogenesis: the formation of the initial central patch of postmitotic cells. *Dev. Biol.* **207**, 309-321.

Hughes, H. and Stephens, D. J. (2008). Assembly, organization, and function of the COPII coat. *Histochem. Cell Biol.* **129**, 129-151.

Humphries, M. M., Rancourt, D., Farrar, G. J., Kenna, P., Hazel, M., Bush, R. A., Sieving, P. A., Sheils, D. M., McNally, N., Creighton, P. et al. (1997). Retinopathy induced in mice by targeted disruption of the rhodopsin gene. *Nat. Genet.* **15**, 216-219.

Jeffery, G. (1998). The retinal pigment epithelium as a developmental regulator of the neural retina. *Eye (Lond.)* **12**, 499-503.

Karan, S., Zhang, H., Li, S., Frederick, J. M. and Baehr, W. (2008). A model for transport of membrane-associated phototransduction polypeptides in rod and cone photoreceptor inner segments. *Vision Res.* **48**, 442-452.

Kimmel, C. B., Warga, R. M. and Schilling, T. F. (1990). Origin and organization of the zebrafish fate map. *Development* **108**, 581-594.

Kondylis, V., Pizette, S. and Rabouille, C. (2009). The early secretory pathway in development: a tale of proteins and mRNAs. *Semin. Cell Dev. Biol.* **20**, 817-827.

Krock, B. L., Bilotta, J. and Perkins, B. D. (2007). Noncell-autonomous photoreceptor degeneration in a zebrafish model of choroideremia. *Proc. Natl. Acad. Sci. USA* **104**, 4600-4605.

Kunte, M. M., Choudhury, S., Manheim, J. F., Shinde, V. M., Miura, M., Chiodo, V. A., Hauswirth, W. W., Gorbatyuk, O. S. and Gorbatyuk, M. S. (2012). ER stress is involved in T17M rhodopsin-induced retinal degeneration. *Invest. Ophthalmol. Vis. Sci.* **53**, 3792-3800.

Lang, M. R., Lapierre, L. A., Frotscher, M., Goldenring, J. R. and Knapik, E. W. (2006). Secretory COPII coat component Sec23a is essential for craniofacial chondrocyte maturation. *Nat. Genet.* **38**, 1198-1203.

Longbottom, R., Fruttiger, M., Douglas, R. H., Martinez-Barbera, J. P., Greenwood, J. and Moss, S. E. (2009). Genetic ablation of retinal pigment epithelial cells reveals the adaptive response of the epithelium and impact on photoreceptors. *Proc. Natl. Acad. Sci. USA* **106**, 18728-18733.

Malicki, J., Neuhauss, S. C., Schier, A. F., Solnica-Krezel, L., Stemple, D. L., Stainier, D. Y., Abdelilah, S., Zwartkruis, F., Rangini, Z. and Driever, W. (1996). Mutations affecting development of the zebrafish retina. *Development* **123**, 263-273.

Marmorstein, A. D. (2001). The polarity of the retinal pigment epithelium. *Traffic* **2**, 867-872.

Marmorstein, A. D., Finnemann, S. C., Bonilha, V. L. and Rodriguez-Boulan, E. (1998). Morphogenesis of the retinal pigment epithelium: toward understanding retinal degenerative diseases. *Ann. N. Y. Acad. Sci.* **857**, 1-12.

Matsuoka, K., Orci, L., Amherdt, M., Bednarek, S. Y., Hamamoto, S., Schekman, R. and Yeung, T. (1998). COPII-coated vesicle formation reconstituted with purified coat proteins and chemically defined liposomes. *Cell* **93**, 263-275.

Matsuoka, K., Schekman, R., Orci, L. and Heuser, J. E. (2001). Surface structure of the COPII-coated vesicle. *Proc. Natl. Acad. Sci. USA* **98**, 13705-13709.

Mazelova, J., Ransom, N., Astuto-Gribble, L., Wilson, M. C. and Deretic, D. (2009). Syntaxin 3 and SNAP-25 pairing, regulated by omega-3 docosahexaenoic acid, controls the delivery of rhodopsin for the biogenesis of cilia-derived sensory organelles, the rod outer segments. *J. Cell Sci.* **122**, 2003-2013.

Murray, A. R., Fliesler, S. J. and Al-Ubaidi, M. R. (2009). Rhodopsin: the functional significance of asn-linked glycosylation and other post-translational modifications. *Ophthalmic Genet.* **30**, 109-120.

Niu, X., Gao, C., Jan Lo, L., Luo, Y., Meng, C., Hong, J., Hong, W. and Peng, J. (2012). Sec13 safeguards the integrity of the endoplasmic reticulum and organogenesis of the digestive system in zebrafish. *Dev. Biol.* **367**, 197-207.

O'Donnell, J., Maddox, K. and Stagg, S. (2011). The structure of a COPII tubule. *J. Struct. Biol.* **173**, 358-364.

Söderström, K.-O., Parvinen, L.-M. and Parvinen, M. (1977). Early detection of cell damage by supravital acridine orange staining. *Experientia* **33**, 265-266.

Ray, A., Sun, G. J., Chan, L., Grzywacz, N. M., Weiland, J. and Lee, E. J. (2010). Morphological alterations in retinal neurons in the S334ter-line3 transgenic rat. *Cell Tissue Res.* **339**, 481-491.

Raymond, S. M. and Jackson, I. J. (1995). The retinal pigmented epithelium is required for development and maintenance of the mouse neural retina. *Curr. Biol.* **5**, 1286-1295.

Robu, M. E., Larson, J. D., Nasevicius, A., Beiraghi, S., Brenner, C., Farber, S. A. and Ekker, S. C. (2007). p53 activation by knockdown technologies. *PLoS Genet.* **3**, e78.

Rosenfeld, P. J., Cowley, G. S., McGee, T. L., Sandberg, M. A., Berson, E. L. and Dryja, T. P. (1992). A *Null* mutation in the rhodopsin gene causes rod photoreceptor dysfunction and autosomal recessive retinitis pigmentosa. *Nat. Genet.* **1**, 209-213.

Saliba, R. S., Munro, P. M., Luthert, P. J. and Cheetham, M. E. (2002). The cellular fate of mutant rhodopsin: quality control, degradation and aggresome formation. *J. Cell Sci.* **115**, 2907-2918.

Schmidt, K. and Stephens, D. J. (2010). Cargo loading at the ER. *Mol. Membr. Biol.* **27**, 398-411.

Schmitt, E. A. and Dowling, J. E. (1994). Early-eye morphogenesis in the zebrafish, *Brachydanio rerio*. *J. Comp. Neurol.* **344**, 532-542.

Schmitt, E. A. and Dowling, J. E. (1999). Early retinal development in the zebrafish, *Danio rerio*: light and electron microscopic analyses. *J. Comp. Neurol.* **404**, 515-536.

Shinde, V. M., Sizova, O. S., Lin, J. H., LaVail, M. M. and Gorbatyuk, M. S. (2012). ER stress in retinal degeneration in S334ter Rho rats. *PLoS ONE* **7**, e33266.

Shiragami, C., Matsuo, T., Shiraga, F. and Matsuo, N. (1998). Transplanted and repopulated retinal pigment epithelial cells on damaged Bruch's membrane in rabbits. *Br. J. Ophthalmol.* **82**, 1056-1062.

Siniossoglou, S., Wimmer, C., Rieger, M., Doye, V., Tekotte, H., Weise, C., Emig, S., Segref, A. and Hurt, E. C. (1996). A novel complex of nucleoporins, which includes Sec13p and a Sec13p homolog, is essential for normal nuclear pores. *Cell* **84**, 265-275.

Stagg, S. M., Gürkan, C., Fowler, D. M., LaPointe, P., Foss, T. R., Potter, C. S., Carragher, B. and Balch, W. E. (2006). Structure of the Sec13/31 COPII coat cage. *Nature* **439**, 234-238.

Stagg, S. M., LaPointe, P., Razvi, A., Gürkan, C., Potter, C. S., Carragher, B. and Balch, W. E. (2008). Structural basis for cargo regulation of COPII coat assembly. *Cell* **134**, 474-484.

Stiemke, M. M., Landers, R. A., al-Ubaidi, M. R., Rayborn, M. E. and Hollyfield, J. G. (1994). Photoreceptor outer segment development in *Xenopus laevis*: influence of the pigment epithelium. *Dev. Biol.* **162**, 169-180.

Strauss, O. (2005). The retinal pigment epithelium in visual function. *Physiol. Rev.* **85**, 845-881.

Sumanas, S. and Larson, J. D. (2002). Morpholino phosphorodiamidate oligonucleotides in zebrafish: a recipe for functional genomics? *Brief. Funct. Genomic. Proteomic.* **1**, 239-256.

Tan, E., Wang, Q., Quiambao, A. B., Xu, X., Qtaishat, N. M., Peachey, N. S., Lem, J., Fliesler, S. J., Pepperberg, D. R., Naash, M. I. et al. (2001). The relationship between opsin overexpression and photoreceptor degeneration. *Invest. Ophthalmol. Vis. Sci.* **42**, 589-600.

Townley, A. K., Feng, Y., Schmidt, K., Carter, D. A., Porter, R., Verkade, P. and Stephens, D. J. (2008). Efficient coupling of Sec23-Sec24 to Sec13-Sec31 drives COPII-dependent collagen secretion and is essential for normal craniofacial development. *J. Cell Sci.* **121**, 3025-3034.

Townley, A. K., Schmidt, K., Hodgson, L. and Stephens, D. J. (2012). Epithelial organization and cyst lumen expansion require efficient Sec13-Sec31-driven secretion. *J. Cell Sci.* **125**, 673-684.

Tsujikawa, M. and Malicki, J. (2004). Genetics of photoreceptor development and function in zebrafish. *Int. J. Dev. Biol.* **48**, 925-934.

Westerfield, M. (2000). *The Zebrafish Book: A Guide For The Laboratory Use Of Zebrafish (Danio Rerio)*. Eugene (OR): University of Oregon Press.

Woo, K. and Fraser, S. E. (1995). Order and coherence in the fate map of the zebrafish nervous system. *Development* **121**, 2595-2609.

Young, R. W. (1967). The renewal of photoreceptor cell outer segments. *J. Cell Biol.* **33**, 61-72.

Zanetti, G., Pahuja, K. B., Studer, S., Shim, S. and Schekman, R. (2012). COPII and the regulation of protein sorting in mammals. *Nat. Cell Biol.* **14**, 20-28.